OPTIMIZATION ANALYSIS FOR LOUVER-FINNED HEAT EXCHANGERS

Jiin-Yuh Jang, Professor ,Department of Mechanical Engineering,
National Cheng Kung University, Tainan, Taiwan 70101,
Bing-Ze Li, graduate student,,Department of Mechanical Engineering,
National Cheng Kung University, Tainan, Taiwan 70101,

Abstract: A series of 3-D computational fluid dynamics analyses along with the simplified conjugate-gradient method were carried out to study the thermal-hydraulic characteristics for the louver-finned heat exchanger. The effects of different louver angles (θ = 20° to 28°), and louver pitches (L_p = 0.8 to 1.2 mm) on the heat transfer phenomenon and pressure drop (in terms of Colburn *j* factor and friction *f* factor) were investigated in detail. The optimization of the louver angle and louver pitch is carried out by using the simplified conjugate-gradient method. The area reduction ratio using a louver fin relative to the plain surface is the objective function to be maximized. The numerical results showed that both the *f* and *j* factors are increased with the increase of the louver angle; while, for a given louver angle, as the louver pitch (L_p) is creased, both the *f* and *j* factors are increased. It is also found that, under the optimum conditions, the area reduction ratio could reach up to 28 % to 37% with Reynolds number (based on the fin pitch) Re_{Fp} ranging from 400 to 1600.

Key Words: optimization, Louver- fin , louver angle and louver pitch

1 INTRODUCTION

Finned-tube heat exchangers are widely used in the air-conditioning industry. To enhance the heat transfer, interrupted surfaces like louver fins are often used. Generally, louver fins are employed since they can increase the heat transfer area and interrupt the development of boundary layers, thus providing higher average heat transfer coefficients and thermal performance.

The topic of louver fins has been studied experimentally with the first reliable data published by Kays and London (Kays and London, 1950). Davenport carried out smoke trace studies on a ten-times scale model and discussed the effects of different geometrical parameters on the heat transfer and pressure drops (Davenport 1983). Achaichia and Cowell made a comprehensive study of louvered plate fin heat exchangers and found the correlations for heat transfer and pressure drops (Achaichia and Cowell, 1988). Webb and Trauger performed flow visualization tests and defined the term "flow efficiency" as the ratio of actual transverse distance to ideal transverse distance (Webb and Trauger, 1991). They also found that the flow efficiency at a given Reynolds number is increased as the louver-to-pitch ratio is reduced. Webb and Jung presented experimental data for six brazed aluminum heat exchangers and found that this design gives a 90% higher heat transfer coefficient for only 25% higher pressure drop compared with the round tube plain plate fin design (Webb and Jung, 1992). Rugh et al. experimentally studied a high fin density louvered surface (Rugh et al., 1992). They reported that the louver fins produce a 25% increase in heat transfer coefficient and 10% increase in pressure drop. Chang and Wang developed the heat transfer and friction correlations, based on the huge data base with 91samples of flat tube heat exchangers (Chang and Wang, 1997). Wang et al. developed heat transfer and friction correlations, based on the data bank with 49 samples of round tube heat exchangers, and claimed that 90% of the experimental data were correlated within 15% (Wang et al., 2001).

The design of louver fin has also been studied numerically with CFD techniques. Suga et al. used a rectangular flow domain filled with overlap Cartesian meshes to compute the flow and heat transfer over a finite-thickness fin(Suga et al. 1990). Ikuta et al. used a block-structured mesh for each louver and found good agreement between computed and measured values of overall heat transfer and pressure loss(Ikuta et al., 1990). Recently, Hsieh and Jang proposed successively variable louver angles and carried out a 3-D numerical analysis on thermal-hydraulic characteristics. Their results showed that varying the louver angles can effectively enhance the heat transfer of the heat exchanges (Hsieh and Jang, 2006). Atkinson et al. investigated the 2-D and 3-D flow and heat transfer

phenomenon of louvered finned-tube heat exchangers (Atkinsona et al., 1998). They found that the 3-D models give predictions of overall heat transfer in better agreement with experimental observations. Recently, Hsieh and Jang numerically investigated the optimal design of a louver finned-tube heat exchanger using the Taguchi method (Hsieh and Jang, 2007). The optimal design values for each parameter were all presented. Jang and Tsai used the simplified conjugate-gradient method (SCGM) to find the optimal louver angle of a louver fin heat exchanger (Jang and Tsai., 2007) for a given louver pitch. The search for optimum louver angles ranging from θ = 15° to 45° were carried . However, they did not serach the optimum combnation of louver anale and louve pitch simulatneously. This has motivated the present investigaion.

In the first part of this study, the effects of different louver angles (θ = 20°~28°), and louver pitches (L_p = 0.8~1.2 mm) on the heat transfer phenomenon and pressure drop is investigated using a commercial CFD code CFD-RC. The results are presented in terms of Colburn j factor and friction f factor.In the second part, the optimization of the louver angle and louver pitch is carried out by using the simplified conjugate-gradient method. The area reduction ratio using a louver fin relative to the plain surface is the objective function to be maximized.

2 MATHEMATICAL ANALYSIS

2.1 Governing Equation

Figure 1 describes the physical model and the computational domain.

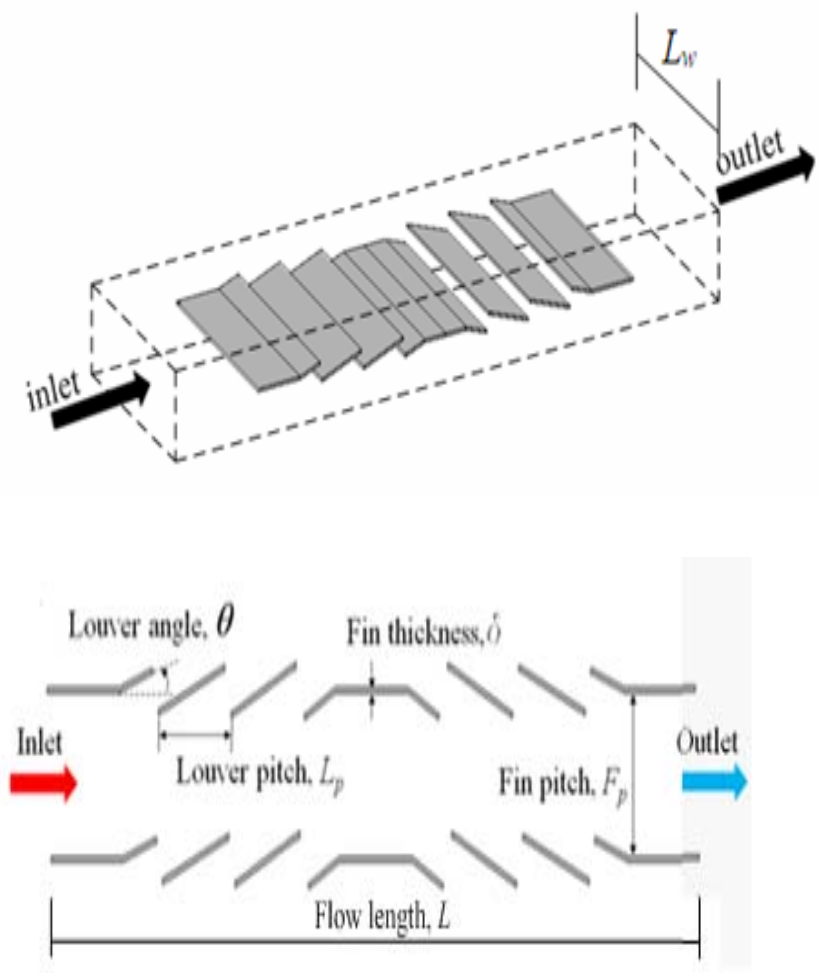

Figure 1 Schematic diagram of computational domain and geometrical parameters

Table 1 The geometry of the physical model

Parameter	Value
fin pitch, F_p	2.7 mm (# 9/inch)
fin thickness,δ	0.1 mm
louver pitch, L_p	0.8 ~ 1.2 mm
louver width, L_w	6.4 mm
louver angle,θ	20° ~ 28°

The relevant geometrical dimensions of the louver fin are also shown in Table 1. The louver angle θ and louver pitch L_p are the main operating parameters in the present study. The relevant numerical results were achieved in the range of 400 <Re_{Fp} < 1600, 20< θ < 28, 0.8 mm < Lp < 1.2 mm. First, we run the the prsent phsical model with 3-D steady laminar and turbulent modes, respectively. The numerical results were compared with those of the experimentas by previous imvestogator (Davenport 1983) as shown in Fig.2. It is found that the fluid may be modelled as a turbulent flow with $\kappa-\varepsilon$ model with reasonably accuracy. Equations for continuity, momentum and energy may be expressed in tensor form：

$$\frac{\partial \overline{u_i}}{\partial x_i} = 0 \tag{1}$$

$$\rho \frac{\partial}{\partial x_j}(\overline{u_i}\,\overline{u_j}) = -\frac{\partial \overline{p}}{\partial x_i} + \mu \nabla^2 \overline{u_i} - \rho \frac{\partial}{\partial x_j}\overline{u_i' u_j'} \tag{2}$$

$$\rho c_p \frac{\partial}{\partial x_j}(\overline{u_j}\,\overline{T}) = k_f \nabla^2 \overline{T} - \rho c_p \frac{\partial}{\partial x_j}\left(\overline{u_j' T'}\right) \tag{3}$$

In the above equations, ρ is fluid density, μ is dynamic viscosity, c_p is heat capacity, and k_f is thermal conductivity of the fluid.The turbulent model adopted here is the $\kappa-\varepsilon$ model：

$$\rho \frac{\partial}{\partial x_j}\left(\overline{u_j}\kappa\right) = \frac{\partial}{\partial x_j}\left[\left(u_l + \frac{u_t}{\sigma_k}\right)\frac{\partial \kappa}{\partial x_j}\right] + \rho(P_r - \varepsilon) \tag{4}$$

$$\rho \frac{\partial}{\partial x_j}\left(\overline{u_j}\varepsilon\right) = \frac{\partial}{\partial x_j}\left[\left(u_l + \frac{u_t}{\sigma_\varepsilon}\right)\frac{\partial \varepsilon}{\partial x_j}\right] + \rho \frac{\varepsilon}{\kappa}[c_1 P_r - c_2 \varepsilon] \tag{5}$$

In the above equations, κ and ε are turbulent kinetic energy and turbulent energy dissipation rate, respectively, defined as

$$\kappa = \frac{1}{2}\overline{(u_i' u_i')} \tag{6}$$

$$\varepsilon = \nu\overline{\left(\frac{\partial u_i'}{\partial x_j}\frac{\partial u_i'}{\partial x_j}\right)} \tag{7}$$

The local Nusselt number is defined as,

$$Nu = \frac{hF_p}{k} = \frac{-\left(\frac{\partial T}{\partial n}\right)_w F_p}{T_w - T_b} \tag{8}$$

where F_p is the fin pitch, T_w is the fin temperature, and T_b is the bulk temperature, which is expressed as

$$T_b = \frac{\int v \cdot T dA}{\int v dA} \tag{9}$$

The average Nusselt number is given by

$$\overline{Nu} = \frac{\int NudA}{\int dA} \tag{10}$$

The Colburn factor (j) and friction factor(f) are defined as

$$j = \frac{\overline{Nu}}{\mathrm{Re}_{Fp}\,\mathrm{Pr}^{1/3}} \tag{11}$$

$$f = \frac{p_{in} - p}{\frac{1}{2}\rho \cdot V_{in}^{\ 2}} \cdot \frac{F_p}{4L} \tag{12}$$

where Re_{Fp} is defined as

$$\mathrm{Re}_{Fp} = \frac{\rho V_{in} F_p}{\mu} \tag{13}$$

and P_{in} is the inlet pressure, Pr is the Prandtl number, L is the flow length.

2.2 Boundary Condition

At the inlet, the flow velocity V_{in} is assumed to be uniform, and the temperature T_{in} is taken to be 25C. At the fin surfaces, no-slip conditions and constant wall temperature T_w (75C) are specified. Cyclic boundary conditions are set on both the upper and lower boundaries, while symmetric boundary conditions are set on both sides of the domain.

2.3 Performance Evaluation Criteria (PEC)

Many performance evaluation criteria (PEC) have been developed for evaluating the performance of heat exchangers. The VG-1 (variable geometry) performance criteria, as described by Webb(webb, 1994) , represents the possibility of surface area reduction by using enhanced surfaces having fixed heat transfer and pumping power.

$$\frac{hA}{h_{plain}A_{plain}} = \frac{j}{j_{plain}}\frac{A}{A_{plain}}\frac{G}{G_{plain}} \tag{14}$$

where the subscript " *ref* " refers to reference plate fin, and G is the mass velocity. The pumping power is calculated as

$$P = (\frac{fA}{A_c}\frac{G^2}{2\rho})(\frac{GA_c}{\rho}) \tag{15}$$

where A_c is the flow area at minimum cross section. The pumping power ratio relative to the reference plane fin can be obtained by

$$\frac{P}{P_{plain}} = \frac{j}{j_{plain}}\frac{A}{A_{plain}}\left(\frac{G}{G_{plain}}\right)^3 \tag{16}$$

and by the elimination of the term

$$\frac{\frac{hA}{h_{plain}A_{plain}}}{(\frac{P}{P_{plain}})^{1/3}(\frac{A}{A_{plain}})^{2/3}} = \frac{\frac{j}{j_{plain}}}{(\frac{f}{f_{plain}})^{1/3}} \tag{17}$$

Under the following conditions

$$\begin{cases} Q/Q_{plain} = 1 \\ hA/h_{plain}A_{plain} = 1 \\ P/P_{plain} = 1 \end{cases} \tag{18}$$

we may obtain the area reduction ratio relative to the reference plane fin as

$$\frac{A}{A_{plain}} = \left(\frac{f}{f_{plain}}\right)^{1/2} \left(\frac{j_{plain}}{j}\right)^{3/2} \tag{19}$$

3 NUMERICAL METHOD

The governing equations are solved numerically using a commercial CFD code (CFD-RC, 2012). The numerical methodology is briefly described here. A third-order upwind TVD (total variable diminishing) scheme is used to model the convective terms of the governing equations, while second-order central difference schemes are employed for the viscous and source terms. A grid system of 192,000 grid points is typically adopted in the computation domain. A careful check for the grid-independence of the numerical solutions is made to ensure the accuracy and validity of the numerical results. For this purpose, four grid systems, 61,440, 122,400, 192,000 and 283,360, are tested. The relative error between the solutions for the 192,000 and 283,360 grid systems in the friction factor is within 3%, while the computation time of the 283,360 grid systems is 2 times that of the 192,000 grid system. Considering the computing time, the 192,000 grid system is adopted here. The convergence criterion is satisfied when the residuals of all variables are less than 1.0×10^{-4}.

4 OPTIMIZATION

In the present study, the simplified conjugate-gradient method (Jang and Tsai, 2011) is combined with a finite differential method code (CFD-RC 2012) as an optimizer to search the optimum louver angle (θ) and louver pitch (Lp). The objective function J_{obj} is defined as the maximum area reduction ratio ($1-A/A_{ref}$).

Above all, the SCGM method evaluates the gradient of the objective function, and then it sets up a new conjugate direction for the updated design variables with the help of a direct numerical sensitivity analysis. The initial guess for the value of each search variable is made, and in the successive steps, the conjugate-gradient coefficients and the search directions are evaluated to estimate the new search variables. The solutions obtained from the finite difference method are then used to calculate the value of the objective function, which is further transmitted back to the optimizer for the purpose of calculating the consecutive searching directions. The procedure for applying this method is described in the following：

(1) Generate an initial guess for two design variables (x_1,x_2) – louver angle (θ) and louver pitch (Lp).
(2) Adopt the finite difference method to predict the velocity and temperature fields associated with the latest θ and Lp, and then calculate the objective function $J_{obj}(x_1,x_2)$.
(3) When the value of $J_{obj}(x_1,x_2)$ reaches a maximum, the optimization process is terminated. Otherwise, proceed to step (4).
(4) Determine the gradient functions, $(\partial J_{obj}/\partial x_1)^{(k)}$ and $(\partial_{Jobj}/\partial x_2)^{(k)}$, by applying a small perturbation (Δx_1,Δx_2) to each value of x_1 and x_2, and calculate the corresponding change in objective function (ΔJ_{obj}). Then, the gradient function with respect to each value of the design variables (x_1,x_2) can be calculated by the direct numerical differentiation .
(5) Calculate the conjugate-gradient coefficients $\gamma^{(k)}$, and the search directions, $\xi_1^{(k+1)}$ and $\xi_2^{(k+1)}$, for each search variable.
(6) Assign values to the coefficients of descent direction (β_1, β_2) for both values of the design variables (x_1, x_2). Specifically, those values are chosen by a trial-and-error process. In general, the coefficients of descent direction (β_1, β_2) are within a range of 0.01 to 0.001.
(7) Update the design variables with

$$x_1^{(k+1)} = x_1^{(k)} + \beta_1 \xi_1^{(k)} \text{ and } x_2^{(k+1)} = x_2^{(k)} + \beta_2 \xi_2^{(k)} \tag{23}$$

5 RESULTS AND DISCUSSION

The present study mainly evaluated the influences of louver angle (θ) and louver pitch (Lp) on the local and overall flow and heat transfer characteristics of louver fin. Furthermore, optimization analyses were utilized in order to search the optimum combination of (θ, Lp) and maximum objective function ($1 - A/A_{ref}$). Figure 2 shows the comparisons of j and f factors between the present numerical

results and the previous imvestogator (Davenport 1983). The present results showed good agreements within a maximum of 16% discrepancy.

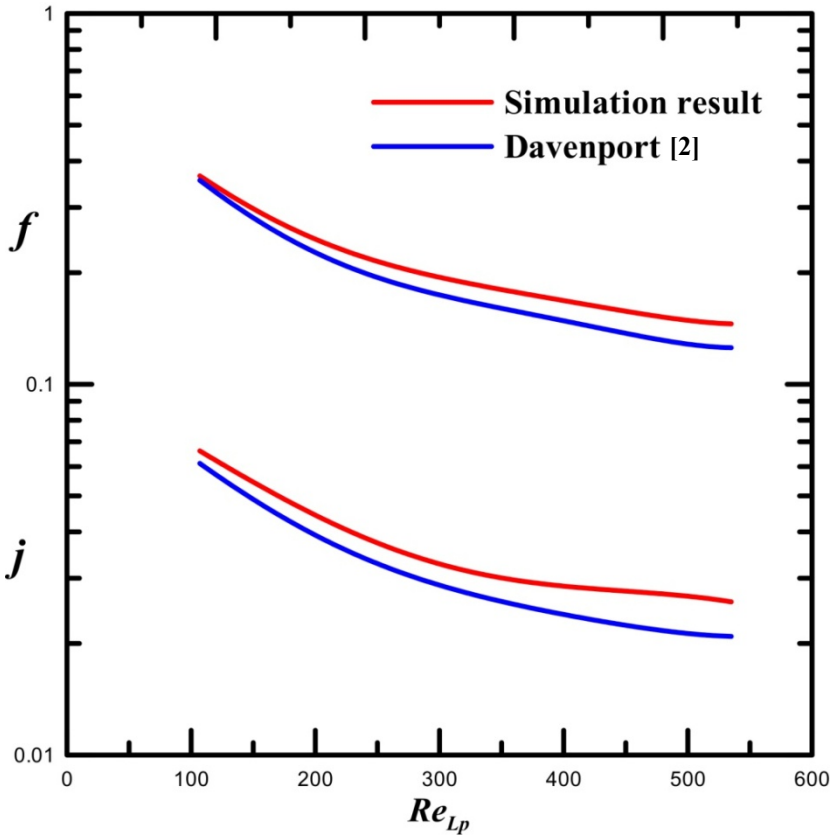

Figure 2 Comparison of the *j* and *f* factors for the present study and previous literature

Figure 3 shows the comparison of streamline distributions for different louver angles at Re_{Fp}=400, L_p =1.00 mm. It can be seen that, at θ = 20°, the streamline of the fluid is quite smooth and much of the fluid flows through the channels between the fins rather than through the louvers. On the other hand, at θ = 28°, the flow is diverted through the louver passages, which is so called "louver directed" flow.

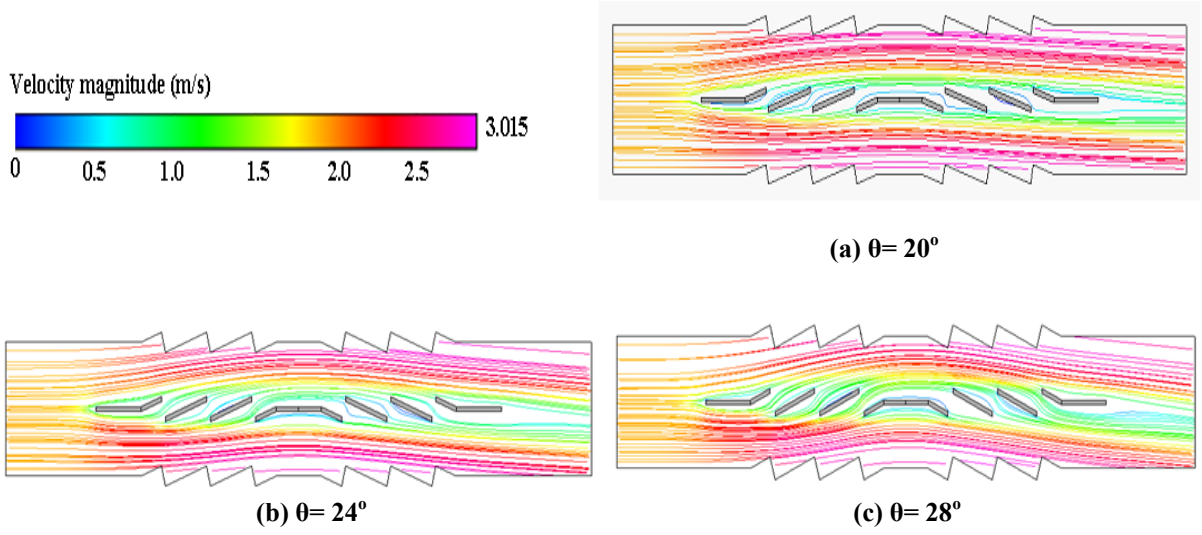

(a) θ= 20°

(b) θ= 24° **(c) θ= 28°**

Figure 3 Streamline distributions at Re_{Fp} = 320 and L_p = 1.00 mm：
(a)θ= 20°, (b)θ= 24 °, (c)θ= 28°

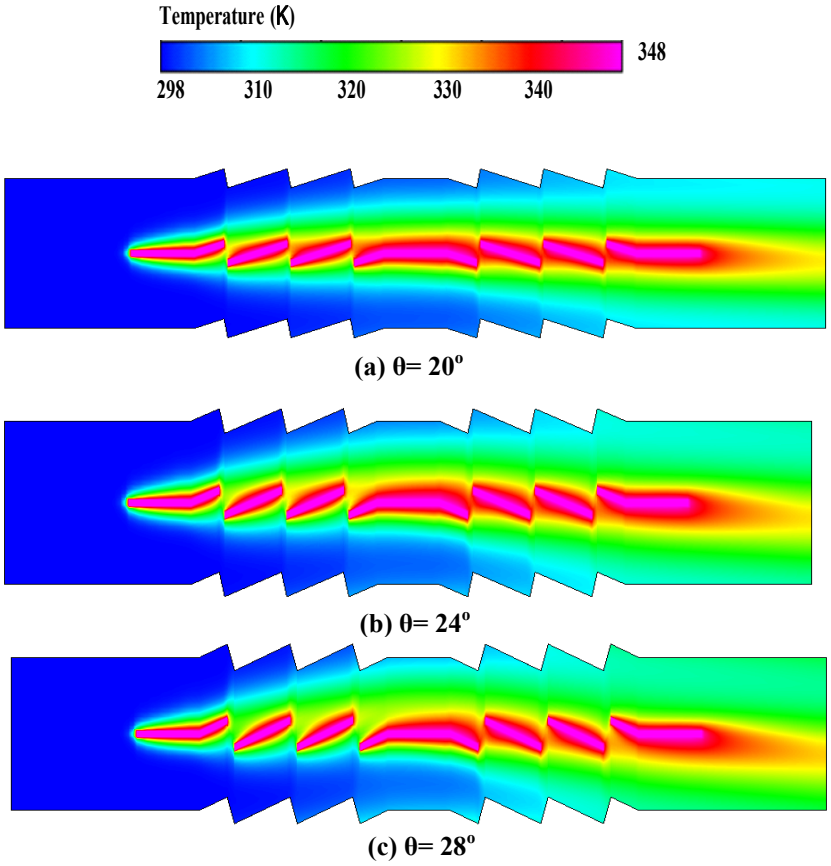

Figure 4 Isotherms at Re_{Fp} = 320 and L_p = 1.00 mm：(a)θ= 20°, (b)θ= 24°, (c)θ= 28°

Figure 4 shows the comparison of temperature distributions for different louver angles. At θ = 28°, the temperature at outlet is higher because of the intensified turbulence, which means the performance of heat transfer is better.The friction factor f and the Colburn factor j versus Re_{Fp} with various louver angles are shown in Figure 5. As the louver angle is increased, both the j and f are increased. For the present study, when the louver angle is increased from 20° to 28°, the values of f is increased by 36.80%, while the values of j is increased by 28.66%, across the Re_{Fp} range (400-1600).

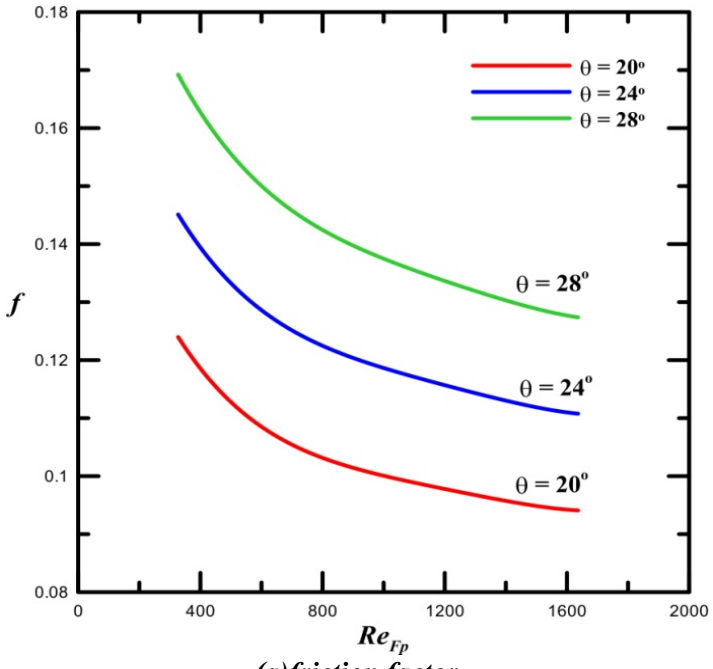

(a)friction factor

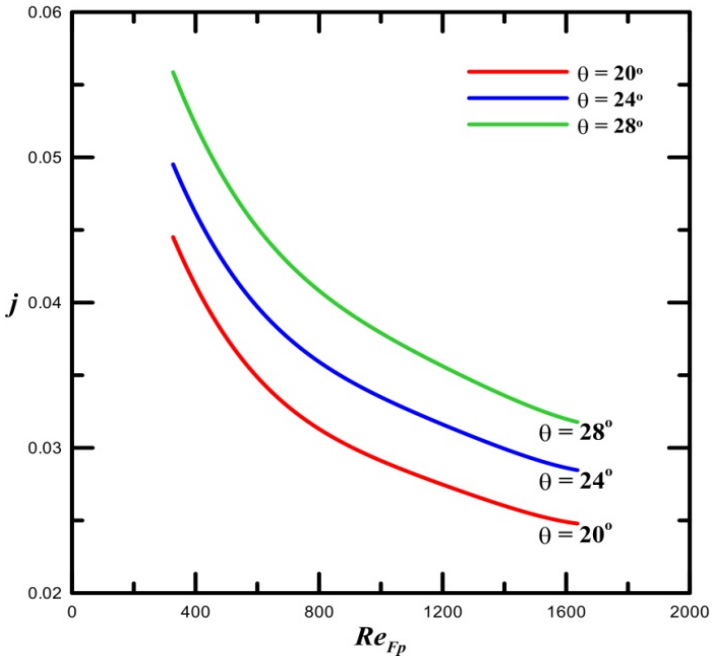

(b) *Colburn factor*

Figure 5 Variations of *f* and *j* factors versus Re_{Fp} with different louver angles

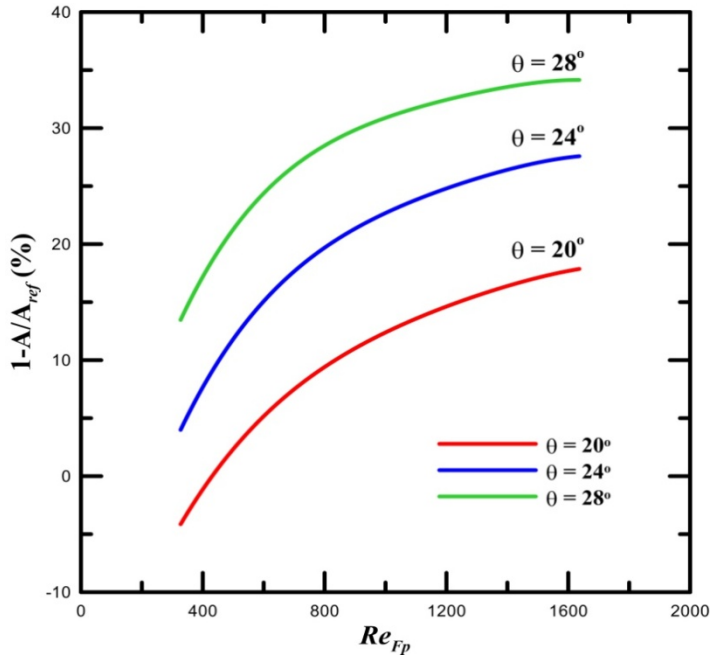

Figure 6 The area reduction ratio versus Re_{Fp} for different louver angles

The area reduction ratios relative to the plain fin surfaces, $1- A/A_{ref}$, for different louver angles are presented in Figure 6. It is shown that the area reduction ratio is increased as the louver angle is increased. For example, at Re_{Fp} = 800, the area reduction ratios for θ = 20° to 24° and 28° are 9.60%, 19.26% and 27.43%, respectively.

The friction factor *f* and the Colburn factor *j* versus Re_{Fp} with various louver pitches are shown in Figure 7. As the louver pitch is increased, both *j* and *f* are increased. For the present study, when the louver pitch is increased from 0.8 mm to 1.2mm, the values of *f* is increased by 2.33%, while the values of *j* is increased by 4.20%, across the Re_{Fp} range (400-1600).

The area reduction ratios relative to the plain fin surfaces, $1- A/A_{ref,}$ for different louver pitches are presented in Figure 8. It is shown that the area reduction ratio is increased as L_p is increased.

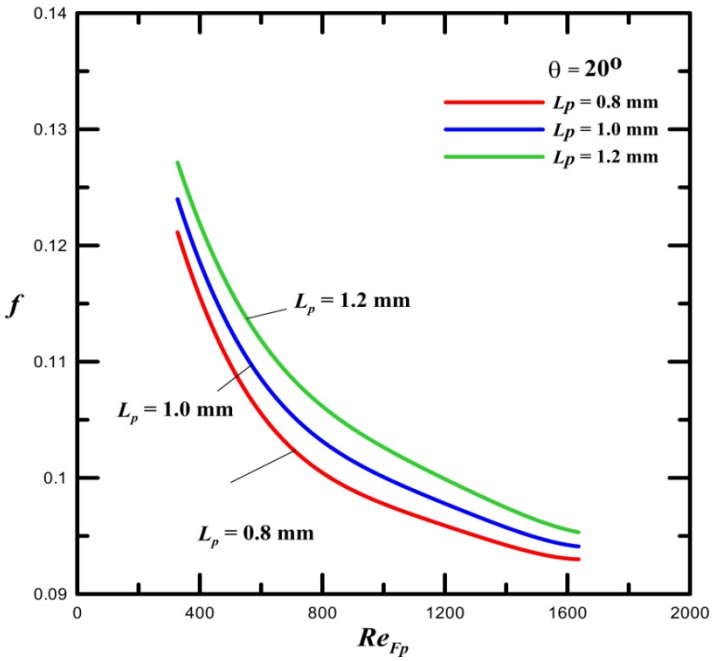

(a) friction factor

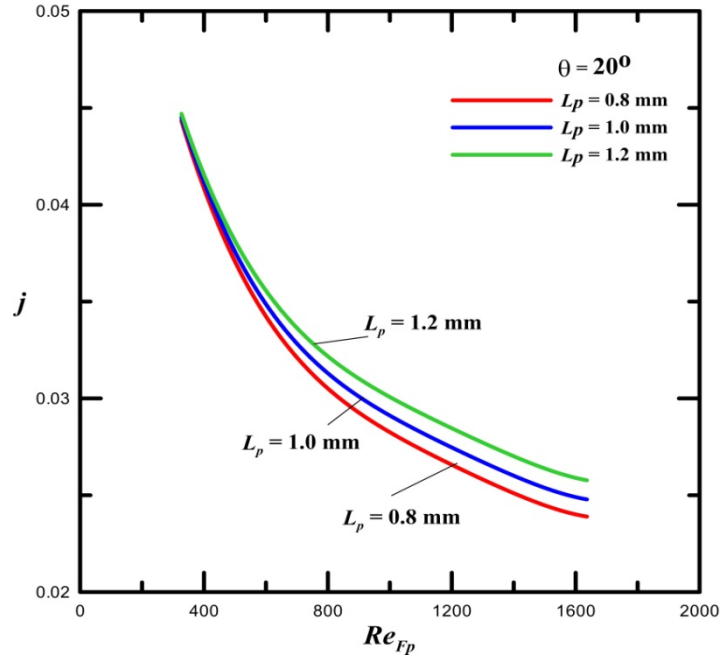

(b) Colburn factor

Figure 7 Variations of *f* and *j* factors versus Re_{Fp} with different louver pitches

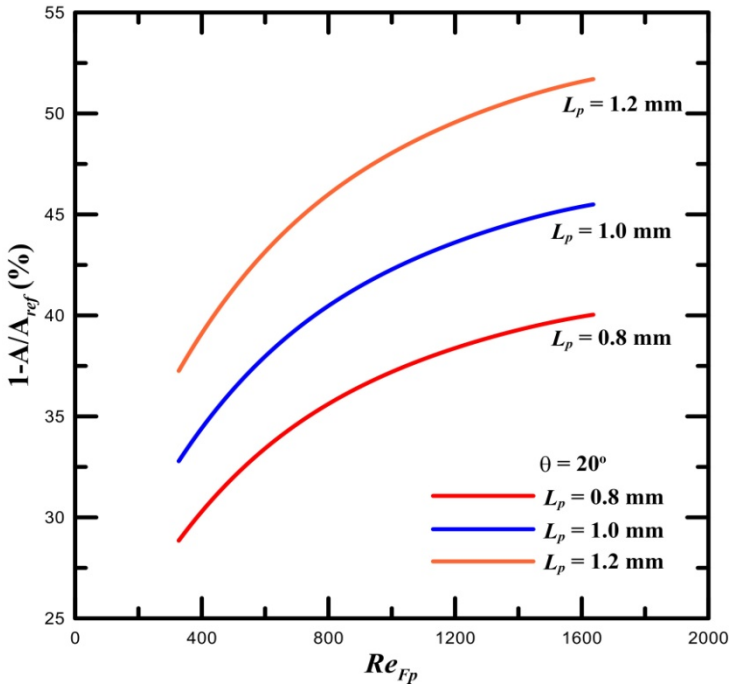

Figure 8 The area reduction ratio versus Re_{Fp} for different louver pitches

Figure 9 displays the iteration process used to search the optimum combination of louver angle (θ) and louver pitch (Lp) for the maximization of objective function(i.e. area reduction ratio, 1-$A/Aref$) at Re_{Fp} = 400 and 1600. The constant area reduction ratio contours are plotted as a function of θ and Lp, where the dark red area represents the maximum area reduction ratio. It is seen that, with the initial values (θi = 35° ,Lpi = 1.2mm) by using the simple conjugated gradient method (SCGM), the optimal θ and Lp combination is obtained for around 33 and 57 iterations, respectively. Thus, the current optimization method provides a tremendous savings in regard to computational time.For Re_{Fp} = 400, the optimal θ and Lp combination are obtained (θ = 33.55° , Lp = 0.84mm) and the area reduction ratio is 27.64%. For Re_{Fp} = 1600, the optimal θ and Lp combination are (θ = 22.3° , Lp = 1.022 mm) and the area reduction ratio is 36.76%.

The searched optimum combination of θ and Lp for louver fin with specific values of Re_{Fp} = 400, 600, 800, 1000, 1200 and 1600 are tabulated in Table 2. It is seen that, the area reduction ratio of 27.64% to 36.76% is achieved across the range of $Re_{Fp.}$ = *400 to 1600.*

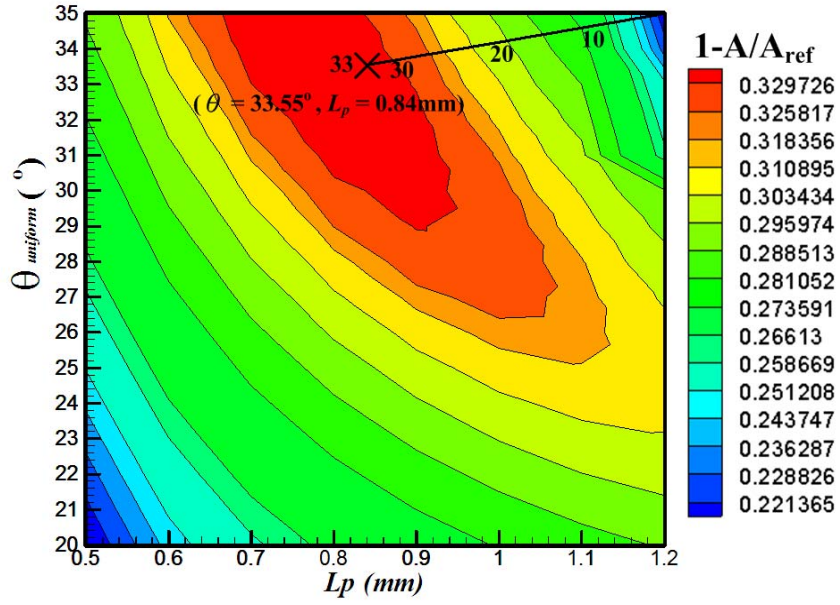

(a) Re_{Fp}=400

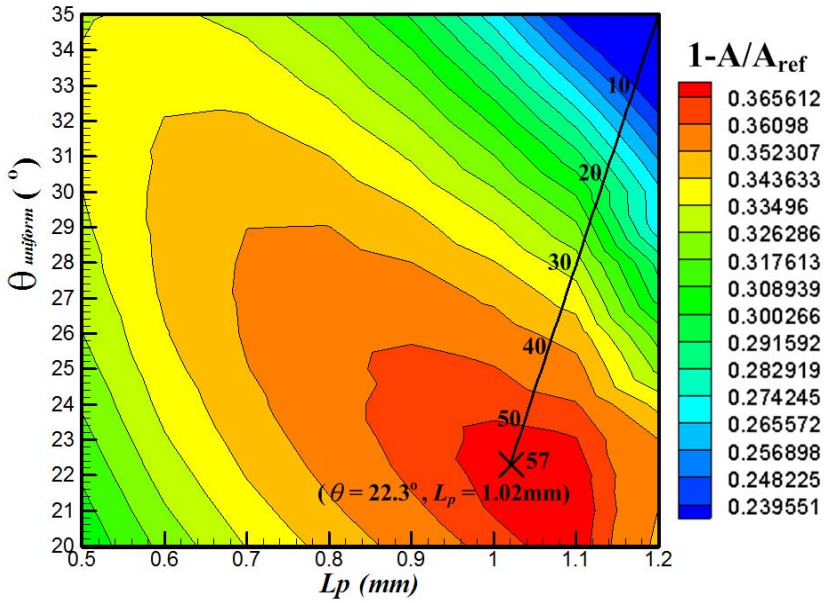

(b)Re_{Fp}=1,600

Figure 9 Iteration process to search the optimum combination of θ and Lp

Table 2 The searched optimum combination of θ and Lp for different Re_{Fp}

Re_{Fp}	L_p (mm)	θ(°)	Area reduction ratio (%)
400	0.84	33.55	27.64
600	0.88	24.15	29.24
800	0.94	23.91	35.40
1000	1.00	23.25	36.19
1200	1.02	23.09	36.55
1400	1.02	22.57	36.73
1600	1.02	22.30	36.76

6 CONCLUSION

Fluid flow and hear transfer for louver-finned heat exchanger were studied numerically. The effects of different louver angles (θ =20° ~ 28°), and louver pitches (L_p = 0.8 ~1.2 mm) on the heat transfer phenomenon and pressure drop were studied in detail. The optimization of the louver angle (θ) and louver pitch (L_p) was performed by using a simplified conjugate-gradient method. A searching procedure for the optimum louver angle (θ) and louver pitch (L_p), ranging from 20° < θ < 35° and 0.5 mm < L_p < 1.2 mm, respectively, was executed. Based on the numerical results, the following conclusions can be drawn：

1. At a fixed louver pitch, as the louver angle (θ) is increased both the j and f factors are increased. For example, as the louver angle is increased from 20° to 28°, the j and f factors are increased by 28.66% and 36.80%, respectively.
2. At a fixed louver angler, as the louver pitch (L_p) is increased, both the j and f factors are increased.
3. The searched optimum objective function associated with an optimal combination of θ and Lp for different Re_{Fp} are obtained for less than 60 iterations. This demonstrates that the current optimization method provides a tremendous savings in regard to computational time for the present physical model. Under the optimum conditions, the area reduction ratio could reach up to 28 % to 37% with Reynolds number ranging from 400 to 1600.

7 ACKNOWLEDGEMENT

Financial support for this work was provided by the National Science Council of Taiwan, under contract NSC 101-2221-E-006-109-MY2

8 REFERENCES

Achaichia, A., T.A. Cowell. 1988. "Heat transfer and pressure drop characteristics of flat tube and louvered plate fin surfaces," *Experimental Thermal and Fluid Science*, vol. 1, pp. 147-157.

Atkinsona, K.N., R. Drakulic, M.R. Heikal, T.A. Cowell. 1998. "Two- and three-dimensional numerical models of flow and heat transfer over louvred fin arrays in compact heat exchangers," *International Journal of Heat and Mass Transfe*r, vol. 41, pp. 4063-4080.

Chang, Y.J., C.C. Wang. 1997. "A generalized heat transfer correlation for Iouver fin geometry," *International Journal of Heat and Mass Transfer,* vol. 40, pp. 533-544.

Davenport, C.L. 1983. "Correlations for heat transfer and flow friction characteristics of louvred fin," *AIChE Symposium Series,* vol. 79, pp. 19-27.

Hsieh, C.T., J.Y. Jang. 2006. "3-D thermal-hydraulic analysis for louver fin heat exchangers with variable louver angle," *Applied Thermal Engineerin*g, vol. 26, pp. 1629-1639.

Hsieh, C.T., J.Y. Jang. 2012. "Parametric study and optimization of louver finned-tube heat exchangers by Taguchi method," *Applied Thermal Engineering,* vol. 42, pp. 101-110.

Ikuta, S., Y. Sasaki, K. Tanaka, M. Takagi, R. Himeno. 1990. "Numerical analysis of heat transfer around louver assemblies," *SAE paper* No.900081.

Jang, J.Y., Y.C. Tsai. 2011. "Optimum louver angle design for a louvered fin heat exchanger," *International Journal of the Physical Sciences* vol. 6, pp. 6422-6438, 2011.

Kays, W.M., A.L. London. 1950. "Heat transfer and flow friction characteristics of some compact heat exchanger surfaces-Part I: Test system and procedure," *ASME Journal of Heat Transfer*, vol. 72, pp. 1075-1085.

Rugh, J.P., J.T. Pearson, S. Ramadhyani. 1992. "A Study of a Very Compact Heat Exchanger Used for Passenger Compartment Heating in Automobiles," *ASME Symposium Series*, vol. 201, pp. 15-24.

Suga, K., H. Aoki, T. Shinagawa. 1990. "Numerical analysis on two-dimensional flow and heat transfer of louvered fins using overlaid grids," *JSME international journal. Ser. 2, Fluids engineering, heat transfer, power, combustion, thermophysical properties*, vol. 33, pp. 122-127.

Wang, C.C., W.S. Lee, W.J. Sheu. 2001 "A comparative study of compact enhanced fin-and-tube heat exchangers," *International Journal of Heat and Mass Transfe*r, vol. 44, pp. 3565-3573.

Webb, R.L., P. Trauger. 1991. "Flow structure in the louvered fin heat exchanger geometry," *Experimental Thermal and Fluid Science,* vol. 4, pp. 205-217.

Webb, R.L., S.H. Jung. 1992. "Air side performance of enhanced brazed aluminum heat exchangers," *ASHRAE Transactions,,* vol. 98, Pt.2, pp. 391-401.

Webb RL, 1994, Principles of Enhanced Heat Transfer*,* New York, John Wiley & Sons